2013

Cation exchange at semiconducting oxide surfaces: Origin of light-induced performance increases in porphyrin dye-sensitized solar cells

Matthew J. Griffith
University of Wollongong, mjg48@uow.edu.au

Kenji Sunahara
Shinshu University

Akihiro Furube
Shinshu University

Attila J. Mozer
University of Wollongong, attila@uow.edu.au

David L. Officer
University of Wollongong, davido@uow.edu.au

See next page for additional authors

Publication Details

Griffith, M. J., Sunahara, K., Furube, A., Mozer, A. J., Officer, D. L., Wagner, P. W., Wallace, G. G. & Mori, S. (2013). Cation exchange at semiconducting oxide surfaces: Origin of light-induced performance increases in porphyrin dye-sensitized solar cells. The Journal of Physical Chemistry C: Energy Conversion and Storage, Optical and Electronic Devices, Interfaces, Nanomaterials, and Hard Matter, 117 (23), 11885-11898.

Cation exchange at semiconducting oxide surfaces: Origin of light-induced performance increases in porphyrin dye-sensitized solar cells

Abstract
The origin of simultaneous improvements in the short-circuit current density (Jsc) and open-circuit voltage (Voc) of porphyrin dye-sensitized TiO2 solar cells following white light illumination was studied by systematic variation of several different device parameters. Reduction of the dye surface loading resulted in greater relative performance enhancements, suggesting open space at the TiO2 surface expedites the process. Variation of the electrolyte composition and subsequent analysis of the conduction band potential shifts suggested that a light-induced replacement of surface-adsorbed lithium (Li+) ions with dimethylpropylimidazolium (DMPIm+) ions was responsible for an increased electron lifetime by decreasing the recombination with the redox mediator. Variation of the solvent viscosity was found to affect the illumination time required to generate increased performance, while similar performance enhancements were not replicated by application of negative bias under dark conditions, indicating the light exposure effect was initiated by formation of dye cation molecules following photoexcitation. The substituents and linker group on the porphyrin chromophore were both varied, with light exposure producing increased electron lifetime and Voc for all dyes; however, increased Jsc values were only measured for dyes containing binding moieties with multiple carboxylic acids. It was proposed that the initial injection limitation and/or fast recombination process in these dyes arises from the presence of lithium at the surface, and the improved injection and/or retardation of fast recombination after light exposure is caused by the Li+ removal by cation exchange under illumination.

Keywords
origin, light, induced, performance, increases, porphyrin, dye, sensitized, solar, cells, oxide, surfaces, semiconducting, exchange, cation

Disciplines
Engineering | Physical Sciences and Mathematics

Publication Details
Griffith, M. J., Sunahara, K., Furube, A., Mozer, A. J., Officer, D. L., Wagner, P. W., Wallace, G. G. & Mori, S. (2013). Cation exchange at semiconducting oxide surfaces: Origin of light-induced performance increases in porphyrin dye-sensitized solar cells. The Journal of Physical Chemistry C: Energy Conversion and Storage, Optical and Electronic Devices, Interfaces, Nanomaterials, and Hard Matter, 117 (23), 11885-11898.

Authors
Matthew J. Griffith, Kenji Sunahara, Akihiro Furube, Attila J. Mozer, David L. Officer, Pawel Wagner, Gordon G. Wallace, and Shogo Mori

Cation Exchange at Semiconducting Oxide Surfaces: The Origin of Light-Induced Performance Increases in Porphyrin Dye-Sensitized Solar Cells

Matthew J. Griffith,[†, ‡,*] Kenji Sunahara,[§] Akihiro Furube,[§] Attila J. Mozer,[†] David L. Officer,[†] Pawel Wagner,[†] Gordon G. Wallace[†] and Shogo Mori [‡,*]

ARC Centre of Excellence for Electromaterials Science and Intelligent Polymer Research Institute, Innovation Campus, University of Wollongong, Northfields Avenue, Wollongong, NSW, 2522, Australia

National Institute of Advanced Industrial Science and Technology (AIST), Tsukuba Central 5, Tsukuba, Ibaraki, 305-8565, Japan.

Division of Chemistry and Materials, Faculty of Textile Science and Technology, Shinshu University, Ueda, Nagano, 386-8567, Japan.

RECEIVED DATE

CORRESPONDING AUTHOR FOOTNOTE

Dr M. Griffith: Faculty of Textile Science and Technology, Shinshu University, Ueda, Nagano, 386-8567, Japan. Telephone: +81 (0)80 4373 3028. Email: mjg48@uow.edu.au

Associate Professor S. Mori: Faculty of Textile Science and Technology, Shinshu University, Ueda, Nagano, 386-8567, Japan. Telephone: +81 (0)268 215 818. Email: shogmori@shinshu-u.ac.jp

[†] ARC Centre of Excellence for Electromaterials Science, University of Wollongong

[§] National Institute of Advanced Industrial Science and Technology (AIST)

[‡] Faculty of Textile Science and Technology, Shinshu University

ABSTRACT

The origin of simultaneous improvements in the short circuit current density (J_{sc}) and open circuit voltage (V_{oc}) of porphyrin dye-sensitized TiO_2 solar cells following white light illumination was studied by systematic variation of several different device parameters. Reduction of the dye surface loading resulted in greater relative performance enhancements, suggesting open space at the TiO_2 surface expedites the process. Variation of the electrolyte composition and subsequent analysis of the conduction band potential shifts suggested that a light-induced replacement of surface-adsorbed lithium (Li^+) ions with dimethylpropylimidazolium ($DMPIm^+$) ions was responsible for an increased electron lifetime by decreasing the recombination with the redox mediator. Variation of the solvent viscosity was found to effect the illumination time required to generate increased performance, whilst similar performance enhancements were not replicated by application of negative bias under dark conditions, indicating the light exposure effect was initiated by formation of dye cation molecules following photo-excitation. The substituents and linker group on the porphyrin chromophore were both varied, with light exposure producing increased electron lifetime and V_{oc} for all dyes, however, increased J_{sc} values were only measured for dyes containing binding moieties with multiple carboxylic acids. It was proposed that there an initial injection limitation and/or fast recombination process in these dyes arises from the presence of lithium at the surface, and the improved injection and/or retardation of fast recombination after light exposure was caused by the Li^+ removal by cation exchange under illumination.

KEYWORDS: porphyrin, dye sensitized solar cells, ion exchange, injection yield, light exposure

INTRODUCTION

Over the last two decades dye-sensitized solar cells (DSSCs) have emerged as an innovative technology for the development of low cost, renewable and environmentally acceptable energy production.[1-3] Efficient charge separation in these devices is achieved by photoinduced electron injection from a sensitizing dye into the conduction band of a metal oxide electrode to which it is chemically anchored. The resulting dye cations are subsequently reduced by a redox electrolyte, which also conducts holes to the cathode. The solar-to-electric power conversion efficiencies of DSSCs depend on a balance of the kinetics for charge injection, collection, recombination and dye regeneration processes,[4] with the best devices currently exhibiting power conversion efficiencies of 11-12 % under AM 1.5 illumination.[5-8]

The efficient light harvesting potential of porphyrins, exemplified by their primary role in photosynthesis, makes them promising candidates for photosensitizers within DSSCs.[7,9] Their synthesis is relatively straightforward, and their optical and electronic properties can be easily tuned via chemical modification of the porphyrin core,[10] the number of porphyrin units,[11,12] and the linker between the core and the inorganic oxide.[13] The capability of porphyrin sensitizers was recently highlighted by a report demonstrating a new DSSC benchmark efficiency of 12.3 % under AM 1.5 full sunlight for a device with a donor–π–acceptor zinc porphyrin sensitizer coupled with a cobalt-based redox mediator.[7] This report demonstrated the remarkable potential of this class of chromophores, although the majority of porphyrin dyes have not approached such impressive efficiencies despite major progress in the development of innovative design strategies.[14-17] It is therefore clearly important that the factors that affect the performance of the porphyrin dyes as sensitizers are systematically elucidated and understood. The most notable limitations for a number of porphyrin dyes include restricted electron injection yields and an enhanced recombination between injected electrons and the acceptor species in the I^-/I_3^- redox mediator.[10,18-20] Strategies to remove such limitations have driven the development of several new

porphyrin dyes,[21-24] however, despite encouraging progress, the reasons for limitations in porphyrin sensitizer performance are not completely understood.

The exposure of DSSCs to light for various time periods has been shown to produce several interesting effects, including performance enhancements and recovery after thermal aging.[25,26] This phenomenon is of great interest due to its considerable practical implications, however, the origin remains ambiguous. Indeed, the behaviour of DSSCs in response to light exposure for time periods ranging from 1 hour to several days is highly dye-dependent. Previous reports have proposed a range of explanations, including enhanced electron transport arising from the creation of shallow TiO_2 electronic states for a ruthenium polypyridyl dye,[26] a positive conduction band shift and photo-production of surface states in the TiO_2 for a perylene dye,[27] or a rearrangement of the dye molecules under illumination for a dendritic oligothiophene ruthenium sensitiser.[28] Recently, a detailed study of this process using time-resolved luminescence on DSSCs prepared with ruthenium complex dyes and various electrolytes determined that the improved J_{sc} observed after light exposure can be attributed to an increased injection yield arising from a change in the kinetics of injection caused by a positive conduction band shift.[29] This paper also reported a reduction in the charge recombination after light exposure to mitigate voltage losses from the conduction band shift. For DSSCs prepared from a zinc porphyrin dye we previously reported that a short light exposure treatment produced simultaneous improvements in the J_{sc}, V_{oc} and fill factor for a zinc porphyrin DSSC. This result could not be completely explained by any of the mechanisms previously reported.[25] Understanding the relationship between dye structure and such effects is essential to design sensitizers for highly efficient DSSCs.

In this report, we investigate the origin of simultaneous improvements, following light exposure, in all photovoltaic performance parameters that we recently reported for porphyrin-sensitized solar cells. Experiments performed to systematically examine the effect of light exposure on the TiO_2 conduction band potential and electron lifetime as a function of (i) dye loading, (ii) electrolyte composition, (iii)

solvent viscosity, and (iv) dye structure, have provided much clearer insight into the principal mechanism responsible for the performance improvements.

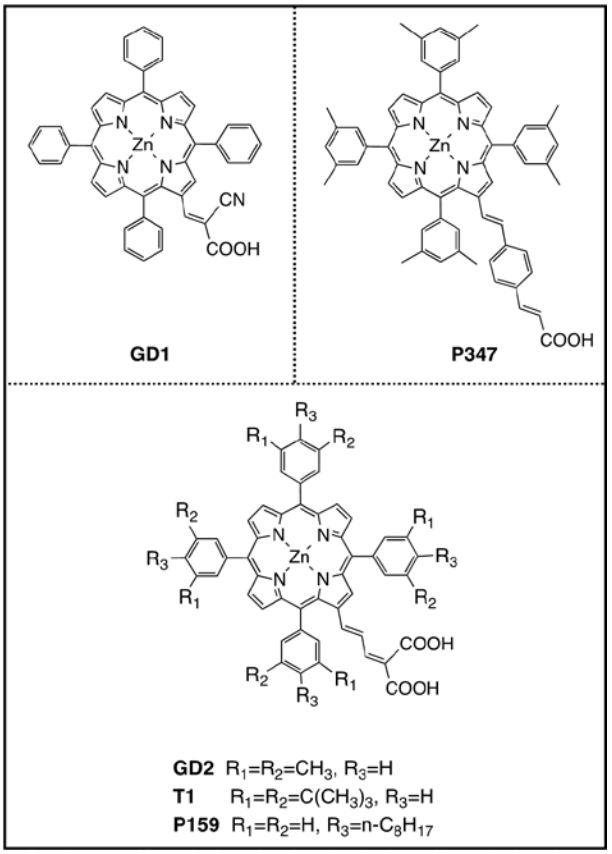

Figure 1. Structures of porphyrin dyes used in this study.

EXPERIMENTAL

Materials. The porphyrin dyes studied here included ***GD1*** [5,10,15,20-tetraphenyl-2-(2-carboxy-2-cyanoethenyl)porphyrinato zinc (II)], ***GD2*** [5,10,15,20-tetra(3,5-dimethylphenyl)-2-(4,4-dicarboxybuta-1,3-dienyl)porphyrinato zinc (II)], ***P159*** [5,10,15,20-tetra(4-n-octylphenyl)-2-(4,4-dicarboxybuta-1,3-dienyl)porphyrinato zinc (II)], ***T1*** [5,10,15,20-tetra(3,5-di-*tert*-butylphenyl)-2-(4,4-dicarboxybuta-1,3-dienyl)porphyrinato zinc (II)] and ***P347*** [5,10,15,20-tetra(3,5-dimethylphenyl)-2-(*p*-(2-carboxyethenyl)styryl)porphyrinato zinc (II)]. The chemical structures of these dyes are displayed in Figure 1. Dye molecules ***GD1***, ***GD2*** and ***P159*** were prepared as previously reported.[11,30,31] The synthesis of porphyrin dyes ***P347*** and ***T1*** will be reported separately.

DSC Fabrication. TiO_2 films were prepared on fluorine-doped tin oxide (FTO) substrates (Asahi Glass Co., Asahi-U, $R_s \leq 12\ \Omega\ sq^{-1}$) using a doctor-blade technique and were sintered at 550°C for 30 minutes in air. The FTO-glass substrates were sonicated in propanol and exposed to UV light and ozone for 15 minutes prior to TiO_2 paste deposition. DSSCs were prepared using a 2.5 μm transparent TiO_2 layer (Nanoxide-T, Solaronix), with film thicknesses measured using a Dektak 150 profilometer. Each film was briefly reheated to 450 $^{\circ}$C before immersion into 0.2 mM anhydrous tetrahydrofuran solutions of porphyrin dyes for 2 hours. Reduced dye loading samples were prepared by sensitization from diluted 0.02 mM anhydrous tetrahydrofuran solutions of porphyrin dyes for 2 hours. Sandwich-type DSSCs were assembled using a 25 μm Hymilan sealant and Pt-sputtered FTO-glass counter electrodes. Electrolyte solutions of varying composition were injected between the electrodes through a hole in the counter electrode, which was subsequently sealed with additional Hymilan. Electrolyte compositions employed in this study included:

I (Standard): 0.6 M 1,2-dimethyl-3-propylimidazolium (DMPImI), 0.5 M 4-tert-butylpyridine (tBP), 0.1 M LiI and 0.05 M I_2 in acetonitrile

II ($DMPIm^+$ rich): 0.7 M DMPImI and 0.05 M I_2 in acetonitrile

III (Li^+ rich): 0.7 M LiI and 0.05 M I_2 in acetonitrile

Light exposure. Light exposure treatments were performed by illumination of the DSSCs with a 100 mW cm^{-2} simulated AM 1.5 light source (YSS-100A, Yamashita Denso) identical to that used for performance characterisation. Light exposure was performed at open circuit for one hour. The temperature of the solar cells during this treatment was not controlled.

DSSC Characterization. Current-voltage curves were recorded using a Keithley 2400 source measure unit after illuminating the DSSCs with a simulated 100 mW cm^{-2} air mass AM 1.5 light source (YSS-100A, Yamashita Denso). The light intensity was adjusted using a calibrated silicon solar cell. The device area was masked with black paint defining an aperture slightly larger than the active area.[32] The light intensity of the simulated sunlight source was reduced for specific measurements using neutral density filters. Incident photon-to-current conversion efficiency (IPCE) spectra were recorded on a set-

up using the monochromated output from a xenon lamp equipped with sorting filters (SM-25, Bunkou, Keiki). The size of the output beam was larger than the DSSC active area. The short circuit current response of devices was recorded in 10 nm steps using a Keithley 2400 source measure unit referenced to the output of a calibrated silicon diode.

Electron Lifetime and Diffusion Coefficient Measurements. Electron lifetimes and diffusion coefficients were determined using stepped-light induced measurements of photocurrent and photo-voltage (SLIM-PCV) transients.[33] Measurements were performed using a 635 nm diode laser (Coherent, LabLaser) illuminating the entire DSSC active area. This wavelength was selected as the dyes are weakly absorbing at 635 nm, allowing a relatively uniform generation of electron density throughout the entire TiO_2 film thickness. The illumination intensity of the laser, controlled by the input voltage, produced values ranging from 1 mW cm^{-2} to 10 mW cm^{-2}. Photocurrent and photovoltage transients were induced by the small stepwise ($\leq$ 10%) change of the laser intensity, controlled with a PC using a digital-to-analogue converter. Induced transients were measured by a fast multimeter (AD7461A, Advantest). Electron densities at each laser illumination intensity were determined by a charge extraction method in which the light source is switched off at the same time as the DSSC is switched from open to short circuit.[34] The resulting current was integrated, with the electron density calculated from the amount of charge extracted. Diffusion coefficients were determined by fitting the current decays to a single exponential as previously reported,[33] although we note that this treatment assumes no recombination losses during charge transport. Electron lifetimes were determined by fitting the voltage transients to single exponential decays as previously reported.[33] The electron diffusion lengths of devices were calculated from transient measurements using a previously reported method where the electron lifetime and diffusion coefficient are determined at the same quasi-static Fermi level.[35] For this purpose the electron lifetime (τ_n) was plotted against the electron density at open circuit and the diffusion coefficient (D_n) was plotted against the electron density at short circuit for identical illumination levels. The short circuit electron density was determined using the previously mentioned charge extraction apparatus; however, no compensating bias was applied to the devices under

illumination. After fitting both trends to power laws, the diffusion length, L_n was calculated as $(\tau_n D_n)^{½}$ for τ and D values computed at the same electron density. The validity of this equation, which assumes a valid linearization of the charge recombination, was checked by determining the order of recombination using semi-logarithmic plots of open circuit voltage versus light intensity and electron lifetime versus open circuit voltage.

RESULTS AND DISCUSSION

I. Dye Loading Variation

GD2 porphyrin-sensitized solar cells were prepared using thin (~2.5 μm) TiO_2 and their current – voltage characteristics immediately recorded. DSSCs were then treated with a one hour light exposure (100 mW cm^{-2} simulated AM 1.5 sunlight) at open circuit and the current – voltage characteristics were re-measured. These results are shown in Figure 2. Device photocurrents were limited compared to our previously reported values[25,30] due to the use of thin TiO_2 films without scattering layers employed in order to avoid possible recombination during charge extraction measurements performed on the same devices. The 1 hour light exposure led to a 6 % increase in the J_{sc} in conjunction with a simultaneous 5 % increase in both the V_{oc} and fill factor, resulting in a 16 % enhancement of the power conversion efficiency. The magnitude of the efficiency enhancement upon light exposure is in close agreement with values we have previously reported for DSSCs prepared with this porphyrin dye.[25] Our previous work on the light exposure effect indicated that heat treatment of devices in the dark produces only small performance improvements, while light treatment using a UV long-pass or IR short-pass filter induces similar improvements to the full simulated AM 1.5 spectrum, suggesting that the effect is linked to the photo-excitation of the porphyrin dye molecules. Accumulation of electrons in the TiO_2 was considered as a possible mechanism for the light exposure effect since the treatment is performed under open circuit conditions where electron density accumulates due to zero extraction. However, accumulating charges by applying a negative bias to the TiO_2 electrode in the dark did not reproduce the same photovoltaic

improvements as the light exposure effects but rather produced the opposite trends in V_{oc} and J_{sc} (see SI, Figure S1). This result, coupled with our previous observations, suggests that photo-oxidation of the dye molecules plays a crucial role in the light exposure effect.

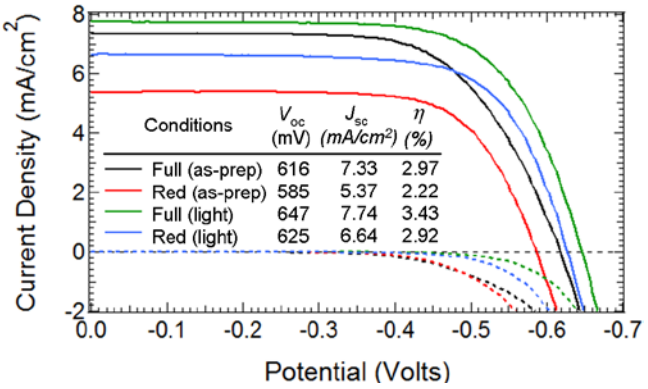

Figure 2. Current density–voltage (*J-V*) curves for full and reduced dye loadings before and after light exposure for ***GD2*** DSSCs. The dark *J-V* curves are shown as dashed lines and the inset displays the photovoltaic performance parameters of each device.

To gain insight into the role of the dye molecule in the light exposure mechanism, the dye surface coverage was reduced by ~50 % by sensitizing films from diluted dye bath solutions. The reduced dye loading DSSCs were then subjected to the same 1 hr light exposure treatment. Current – voltage curves and photovoltaic performance parameters for the reduced dye loadings are also included in Figure 2. Light exposure of the reduced dye devices produced a J_{sc} enhancement of 24 %, a 6 % increase in the V_{oc} and an unchanged fill factor, leading to a 32 % enhancement of the power conversion efficiency. The V_{oc} increase is similar to that observed with full dye surface coverage (6 %), however the light-induced photocurrent enhancement is notably larger, leading to a larger relative increase in the initial device efficiency for the reduced dye device. This result implies that the ratio between the number of dye molecules and electrolyte species plays an important role in the light exposure performance enhancement mechanism.

The role of the dye molecules was examined further by measuring open circuit voltage and short circuit current decays for ***GD2***-sensitized DSSCs with different dye coverages. Electron lifetimes and diffusion coefficients determined before and after 1 hour light exposure are shown for different laser intensities in

Figure 3. The raw transients from which this data is derived are shown in Figures S2-S5 (Supporting Information). Photovoltage decay measurements demonstrate a factor of 2 to 4 increase in the electron lifetime (τ) at matched electron density for the full dye loading after light exposure (Figure 3(b)). Conversely, a decrease in the electron diffusion coefficient (D) at the same electron density was also observed as seen in Figure 3(a). The V_{oc} vs electron density plot exhibits no shift in either the slope or intercept before and after light exposure (Figure 3(c)). Since each device employs an identical redox mediator, this lack of change indicates an identical TiO_2 conduction band level and no change in the trap density or distribution before and after light exposure. The trends in electron lifetime and diffusion coefficients following light exposure are identical for the reduced and full dye loading devices. When the dye loading is reduced, the diffusion coefficients and conduction band potentials remain identical to the sample with full dye loading, however, the electron lifetime is slightly shorter for the reduced dye sample. This is indicative of a physical blocking effect, where decreasing the amount of dye diminishes the blocking effect, allowing I_3^- acceptor species closer to the TiO_2 surface and reducing the electron lifetime through an enhanced probability for recombination.

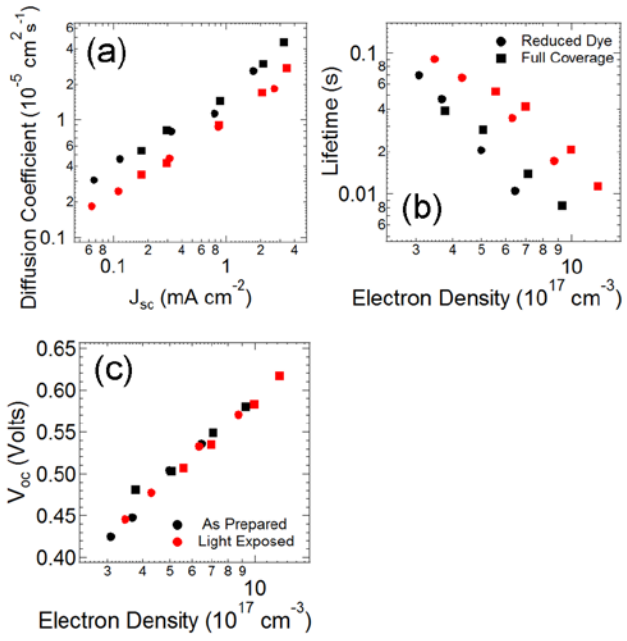

Figure 3. (a) Electron diffusion coefficient vs J_{sc}, (b) electron lifetime vs electron density and (c) V_{oc} vs electron density in the TiO_2 film prior to (black) and following (red) light exposure for ***GD2***-sensitized solar cells with full (squares) and reduced (circles) dye loadings.

To measure electron density in the TiO_2 film accurately, the electron diffusion length in DSSCs must be longer than the thickness of the TiO_2 film employed.[36] It is possible that charge collection losses due to a low diffusion length affect the J_{sc} in these devices. In this case, the increase in J_{sc} observed after light exposure could be due to an increased diffusion length. To check if the thickness of our devices is shorter than the electron diffusion length, the open circuit voltage at matched electron density was compared among DSSCs with a range of different TiO_2 thicknesses (Figure 4(a)). As discussed earlier, the V_{oc} vs log(ED) plot indicates the relative TiO_2 E_{CB} level, which should not be affected by the film thickness. The data measured here shows that the V_{oc} vs log(ED) plots are invariant for both full and reduced dye loadings for film thicknesses between 1.6 μm and 4.5 μm, and confirms the earlier observation that there are minimal shifts after light exposure. However, when the film thickness is increased to 6 μm or higher, the plots begin to show a negative shift, that is, a shift towards higher V_{oc} values at matched electron density. Since it is highly unlikely the TiO_2 conduction band shifts negatively by up to 50 mV simply by increasing the film thickness by 2 μm, this result suggests that there are some recombination losses during charge extraction for the 6 μm films, and thus the electron density was underestimated. This leads to identical V_{oc} values appearing to correlate with a lower charge density due to recombination, which manifests as the observed negative shift on the V_{oc} vs log(ED) plot. This result implies that the diffusion length of these devices is approximately 5 μm at open circuit. However, we note that previous studies of diffusion length have predicted and observed a decrease in diffusion length with decreased electron density.[37,38] This arises due to a typically sub-linear recombination reaction order with respect to the redox mediator. To analyse whether such effects occur in the present porphyrin system, which would further reduce the diffusion length at the lower electron density values found at short circuit, we have computed the diffusion length (L_n) from transient measurements of the electron lifetime and diffusion coefficient. To ensure the same quasi Fermi level for measurements performed at open circuit (lifetime) and short circuit (diffusion coefficient), the

electron density was determined at the appropriate circuit condition for each measurement. The diffusion length was then computed using values computed at identical electron densities using:

$$L_n = (\tau_n D_n)^{1/2} \qquad \text{Equation (1)}$$

These results are shown in Figure 4(b). The diffusion length at open circuit was determined to be 5.6 μm for as prepared devices, and 5.9 μm for light exposed devices from Equation (1). These values are consistent with the data from Figure 4(a) suggesting a diffusion length between 4.5 and 6.2 μm at open circuit. Little change was observed as the electron density decreased, with values of 8.5 μm (as prepared) and 8.3 μm (light exposed) observed at the electron density equating to short circuit conditions under AM 1.5 illumination. The minimal change in diffusion length suggests either the linearity of recombination must be close to unity for these samples, or, alternatively, the subsequent analysis assumptions of linearization of recombination are invalid. The linearity of recombination was investigated by determining both the relationship between V_{oc} and the logarithm of the light illumination, $\log(I_0)$, and the relationship between the logarithm of the lifetime, $\log(\tau_n)$ and the V_{oc}. This data is shown in Figure S6. Slopes of 70-72 mV were observed for the V_{oc} vs $\log(I_0)$ plots, and 12.5-13.3 V^{-1} for the $\log(\tau_n)$ vs V_{oc} plots. Compared to the ideal values of 59 mV and 16.9 V^{-1} respectively, these values yield consistent recombination reaction orders of $\gamma = 0.79$ for as prepared devices and $\gamma = 0.82$ for light exposed devices. Given the recently proposed linearity correction of Bisquert et al, where the diffusion length, λ_n, is given by:

$$\lambda_n = \left(\frac{D_0 \, n_b^{\,1-\gamma} \, \tau_0}{\gamma} \right)^{1/2} \qquad \text{Equation (2)}$$

where D_0 and τ_0 are the free electron diffusion coefficient and lifetime respectively and n_b the background electron density, the diffusion length at short circuit predicted by Equation (2) exhibits a reduction by a factor of 1.4 (as prepared) or 1.3 (light exposed) compared to the value measured at open circuit. By applying these reduction factors to the open circuit diffusion length determined from Equation (1), the diffusion length at short circuit was estimated to be 4.0 μm for as prepared, and 4.5 μm

for light exposed devices. The difference between short circuit values from Equation (1) and Equation (2) may arise from the photocurrent transient measurement technique not providing completely homogeneous electron density generation in the TiO_2 film due to extraction at short circuit as previously reported.[38]

The variation in device J_{sc} with film thickness also aids in estimating the diffusion length at short circuit. Figure 4(c) displays J_{sc} data measured for films of different thickness and normalized to the largest observed value. At one sun intensity, the J_{sc} is observed to increase up to a thickness of 3.4 μm, and then remain constant within error between 3.4 and 6.0 μm. There is then a detectable decrease in J_{sc} when the TiO_2 thickness is increased to 8.2 μm. This result suggests clear charge collection losses at a thickness of 8.2 μm, and a diffusion length in the range of 3.4 μm – 6.0 μm at short circuit. Such an analysis is somewhat oversimplified since the light harvesting efficiency also increases with film thickness and could mask the onset of collection losses. We therefore calculated the J_{sc} expected from each film thickness by first computing the IPCE using LHE = $1 - 10^{-\alpha d}$, where α is the molar absorption coefficient and d the film thickness, then employing an injection efficiency of 0.65 estimated from a previous publication[25] and assuming no collection losses. Since light harvesting is almost quantitative in a 2 μm film in the Soret absorption band due to the high molar extinction coefficient (2×10^5 M^{-1} cm^{-1}), only changes in the IPCE in the red region were computed using an average molar extinction coefficient of 8×10^3 M^{-1} cm^{-1} between 500 nm and 650 nm. The computed IPCE data was then integrated with the solar irradiance spectrum overlap to calculate an expected J_{sc}. These values appear as the yellow trend line in Figure 4(c). The measured J_{sc} increases are consistent with the increases expected from enhanced light harvesting up to 3.4 μm, suggesting no collection losses up to this film thickness. The measured J_{sc} is clearly lower than the predicted value for a 6 μm film, consistent with a short circuit diffusion length of 3.4 – 6 μm, in agreement with the predicted diffusion length at short circuit from Equation (2) and close to the value from Equation (1). Since the data in Figures 4(a)-4(c) collectively confirms that the

short circuit diffusion length is longer than the TiO_2 film thickness of 2.5 μm, it is concluded that changes in charge collection cannot be the origin of the observed device J_{sc} increase after light exposure. Based on these results, the J_{sc} increase after light exposure is attributed to an improvement in charge generation. The exact origin of the improvement could be due either to an improved injection yield, faster injection kinetics, decreased fast recombination, or a combination of these alternatives.

Since our system for measuring voltage and current transients operates at reduced light intensity (maximum value 10 mW cm^{-2}), we also attempted to confirm that the information determined from these measurements could be used to explain trends observed in *J–V* measurements under 100 mW cm^{-2} illumination. For instance, the electron lifetime trends for the reduced dye loading samples in Figure 3(b) appear to be slightly diverging towards larger electron densities, and thus conclusions regarding the diffusion length and negligible charge collection losses determined at 10 mW cm^{-2} may not be valid at 100 mW cm^{-2}. To address this, the average relative increase in the photocurrent observed in four different DSSCs after light exposure was determined for both full and reduced dye loadings under AM 1.5 spectral irradiation at different illumination intensities (Figure 4(d)). This data verifies that the enhanced J_{sc} improvement observed after light exposure for the reduced dye loading samples is consistent within experimental errors at reduced light intensities of 30 mW cm^{-2} and 12 mW cm^{-2}. Figures 4(a) and 4(b) suggest with measurements on the transient system with an illumination power of up to 10 mW cm^{-2} that charge collection losses have little influence on performance in these DSSCs. Since the J_{sc} increases appear similar at 12 mW cm^{-2}, 30 mW cm^{-2} and 100 mW cm^{-2} light intensities, it is concluded that information obtained from the low light intensity source can be used to explain device trends measured under one sun illumination. This is supported by the measurements of J_{sc} at 100 mW cm^{-2} also implying minimal charge collection losses in these devices (Figure 4(c).

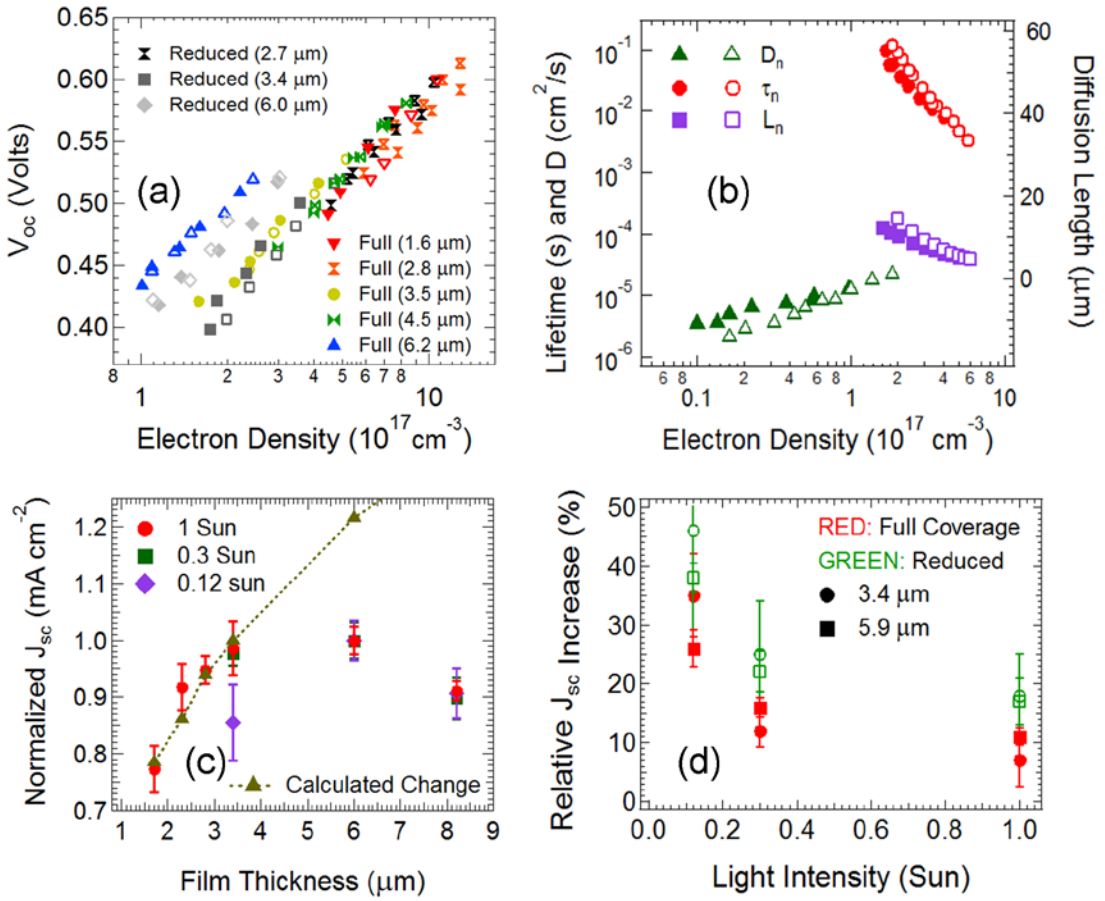

Figure 4: (a) V_{oc} vs electron density in the TiO_2 film prior to (solid symbols) and following (open symbols) light exposure for ***GD2***-sensitized solar cells prepared with various film thicknesses. (b) Electron diffusion length calculated as $(D_n \tau_n)^{½}$ prior to (solid symbols) and following (open symbols) light exposure for devices with full dye loading. (c) Dependence of normalized J_{sc} on film thickness for different illumination intensities. The J_{sc} predicted from calculated IPCE changes is shown in yellow. and (d) Relative improvement in the J_{sc} following light exposure for reduced (green) and full (red) dye loading at various illumination intensities. Measurements were performed for DSSCs prepared from 3.4 μm (circles) and 5.9 μm (squares) TiO_2 films.

II. Variation of the Electrolyte Composition

Influence on *J–V* Characteristics

The nature of the cations employed in the electrolyte is known to have a significant impact on charge transfer processes in DSSCs,[39-41] and may therefore effect the light exposure mechanism. To investigate the influence of electrolyte components on the light exposure mechanism, DSSCs were prepared with three different electrolyte compositions: a standard mixture (I), a dimethylpropylimidazolium ($DMPIm^+$)-rich electrolyte, which contained no lithium or *tert*-butylpyridine (II), and a lithium-rich electrolyte which employed no $DMPIm^+$ or *tert*-butylpyridine (III). The ionic strength of the cations was

maintained at 0.7 M in all cases. The *J-V* curves for DSSCs constructed from each electrolyte prior to and following a light exposure treatment are shown in Figure 5, with the photovoltaic performance parameters of these devices reported in Table 1.

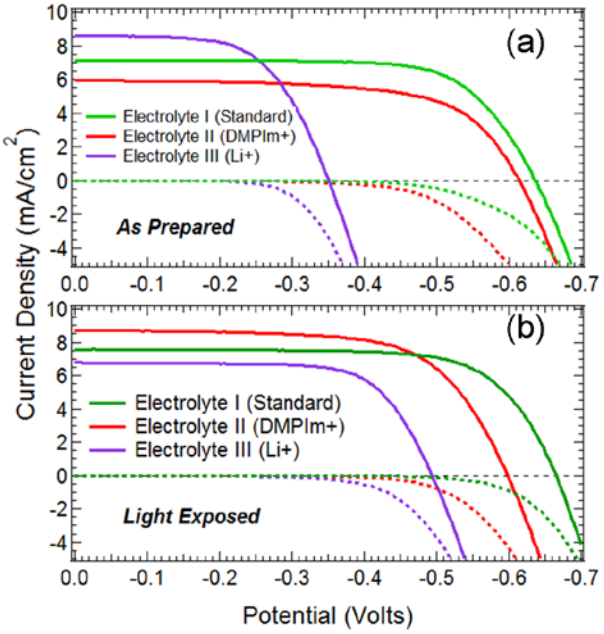

Figure 5. Current density–voltage curves for (a) as-prepared and (b) light exposed DSSCs prepared from porphyrin dye ***GD2*** with three different electrolyte compositions.

Figure 5(a) shows that the V_{oc} and J_{sc} for as-prepared devices made with the $DMPIm^+$ electrolyte were both lower than those prepared with the standard electrolyte. As-prepared devices constructed from the Li^+ electrolyte exhibited a significantly reduced V_{oc} but produced a higher J_{sc} than those prepared with the standard electrolyte. After light exposure, Figure 5(b) demonstrates that the standard electrolyte device exhibited a 5 % increase in the V_{oc} with a simultaneous 5 % increase in the J_{sc}. In contrast, light exposure reduced the V_{oc} by 3 % in the $DMPIm^+$ device, however the J_{sc} was increased by 47 %. The devices containing the Li^+ electrolyte exhibited a 41 % increase in the V_{oc} after light exposure accompanied by a corresponding 21 % reduction in the J_{sc}.

Electron lifetimes and diffusion coefficients derived from transient photocurrent and photovoltage measurements are presented in Figure 6. The raw transients from which data is derived for Electrolyte

II and III are shown in Figures S7-S10 (Supporting Information). The transients for the sample in standard electrolyte I were very similar to those shown earlier for a previous sample (Figure S2-S3) and are thus not reproduced.

Table 1. Photovoltaic parameters measured before and after light exposure for ***GD2*** DSSCs prepared using electrolytes I, II, and III

Electrolyte	V_{oc} (mV)		J_{sc} (mA/cm^2)		Fill Factor		η (%)	
	As Prepared	Light Exposed	As Prepared	Light Exposed	As Prepared	Light Exposed	As Prepared	Light Exposed
I (Standard)	634	665	7.12	7.57	0.709	0.710	3.20	3.58
II ($DMPIm^+$)	612	598	5.94	8.72	0.653	0.659	2.37	3.44
III (Li^+)	350	494	8.61	6.78	0.601	0.697	1.81	2.34

Figure 6(b) shows that the electron lifetime for the standard electrolyte is higher than that of both other electrolytes, with the $DMPIm^+$ rich electrolyte exhibiting a slightly higher electron lifetime than the Li^+ rich electrolyte at matched electron density. The Li^+ electrolyte also displays the lowest diffusion coefficient, with the $DMPIm^+$ electrolyte exhibiting the highest diffusion coefficient and the standard electrolyte producing a value between these two extremes. The V_{oc} vs electron density plots in Figure 6(c), indicative of the TiO_2 E_{CB} value since the redox mediator concentration and solvent are identical for each electrolyte, demonstrate that devices prepared from the Li^+ electrolyte have the most positive E_{CB}, whilst those prepared from the $DMPIm^+$ electrolyte have the most negative E_{CB}. The standard electrolyte again exhibits an E_{CB} value between these two extremes. Light exposure of these devices produces an increase in the electron lifetime for each electrolyte. Figure 6(a) shows that the diffusion coefficients of the standard and $DMPIm^+$ electrolytes are reduced after light exposure, whilst that of the Li^+ electrolyte is increased. The V_{oc} vs electron density plot indicates that the E_{CB} for the Li^+ electrolyte exhibits a significant negative shift upon light exposure, whilst the $DMPIm^+$ experiences a positive E_{CB} shift with respect to the NHE potential scale. There is no change to the TiO_2 conduction band upon light

exposure of the standard electrolyte as observed in both our previous measurements[25] and those shown earlier in this work (Figure 3). We note that previous reports have suggested light exposure of DSSCs can lead to a change in the trap density of the TiO_2.[26,27,42] The data in Figure 6 indicates that the slope of the V_{oc} vs electron density plots remains constant for the standard electrolyte before and after light exposure, implying that the density of trap states in the semiconductor remains constant. For the Li^+ electrolyte there appears to be little change in slope, whilst for the $DMPIm^+$ electrolyte, there is a small change in the slope. Changes in the slopes of these plots could represent changes in the trap density distribution in the TiO_2. However, the slope divergence is most noticeable at lower energy levels, where the ratio of traps to total trap density is relatively low. Whilst the influence of a change in trap density on the photovoltaic performance cannot be excluded, the trends in $J - V$ data from Table 1 for the case of electrolyte II can be primarily accounted for by shifts in the TiO_2 conduction bands as discussed below.

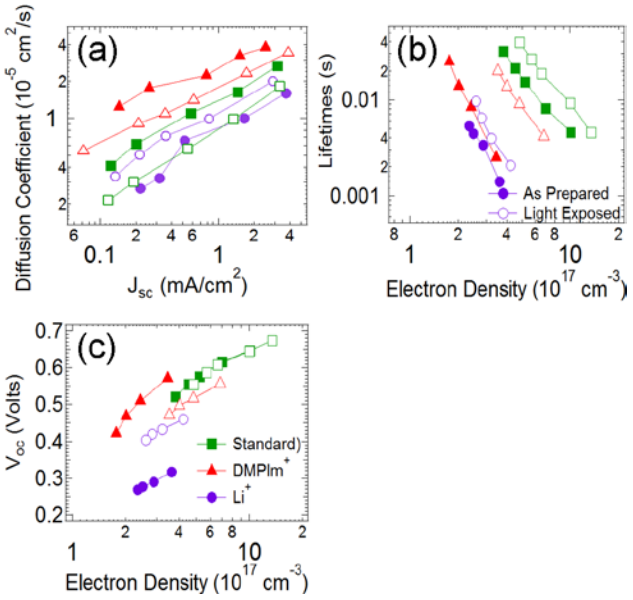

Figure 6. (a) Diffusion coefficient versus J_{sc} (b) electron lifetime versus electron density, and (c) V_{oc} versus electron density before (solid symbols) and after (open symbols) light exposure for ***GD2*** DSSCs sensitized with electrolytes I (green squares), II (red triangles) and III (purple circles)

The light-induced J_{sc} and V_{oc} changes in each device can be largely rationalized based on the changes in the electron lifetime (τ) and E_{CB}. The overall trends in electron lifetime, diffusion coefficients, J_{sc} and V_{oc} in response to light exposure are summarized in Table 2, with possible causes of these trends

discussed in further detail below. For as-prepared devices, the low V_{oc} of the Li^+ electrolyte arises from a combination of a more positive E_{CB} position and the shortest electron lifetime. The $DMPIm^+$ device has a more negative E_{CB}, however, the electron lifetime for this device is shorter than those prepared from the standard electrolyte, resulting in a lower electron density at open circuit, and consequently a lower V_{oc} than the standard electrolyte. The J_{sc} trends are related to the comparative E_{CB} positions since shifts of this energy level directly alter the overlap between the TiO_2 acceptor states and the dye LUMO orbital, often referred to as the driving force for injection (ΔG_{inj}). The Li^+ electrolyte, with the most positive E_{CB} and largest ΔG_{inj} is therefore expected to produce the highest J_{sc}, whilst the $DMPIm^+$ electrolyte, with the most negative E_{CB} and smallest ΔG_{inj} produces the lowest J_{sc}. Following light exposure, the V_{oc} for the Li^+ device increases due to a negative E_{CB} shift and an increased electron lifetime. The $DMPIm^+$ V_{oc} exhibits a reduced V_{oc} due to significant positive E_{CB} shift, somewhat offset by a simultaneous increase in the electron lifetime. It is significant to note that although the J_{sc} trends for each electrolyte seem to be consistent with changes in ΔG_{inj} after light exposure, the J_{sc} for as-prepared devices with the Li^+ electrolyte (8.61 mA cm^{-2}) and light exposed devices using the $DMPIm^+$ electrolyte (8.72 mA cm^{-2}) are almost identical despite a large difference in the E_{CB} for the two cases. Furthermore, comparing devices after light exposure, the Li^+ electrolyte still has a more positive E_{CB} than the $DMPIm^+$, however the J_{sc} for the Li^+ electrolyte (6.78 mA cm^{-2}) is significantly lower. This result cannot be explained by an injection yield that is dominated by the potential difference between the TiO_2 conduction band and the dye LUMO only. One possible explanation for this is that the presence of lithium ions acts to impair the charge generation process, despite increasing the value of ΔG_{inj}.

Table 2. The origin of observed trends in various photovoltaic parameters following light exposure for ***GD2*** DSSCs prepared using electrolytes I, II, and III

Parameter	***Electrolyte I (Standard)***		***Electrolyte II ($DMPIm^+$)***		***Electrolyte III (Li^+)***	
	Trend	***Dominant Cause***	***Trend***	***Dominant Cause***	***Trend***	***Dominant Cause***
D	Decrease	Li^+ partially complexed by tBP, $DMPIm^+$ adsorption effect dominates	Decrease	$DMPIm^+$ adsorbs to TiO_2, less mobile ions and $D_{ambipolar}$ lower	Increase	Adsorbed Li^+ removed, more mobile ions and $D_{ambipolar}$ higher
τ	Increase	Less I_3^- in surface region (Removal of Li^+ and blocking from $DMPIm^+$)	Increase	$DMPIm^+$ surface adsorption blocks I_3^-. Also $\Delta G_{recombine}$ decreased	Increase	Removal of Li^+ from surface also removes I_3^-
J_{sc}	Increase	No change in ΔG_{inj}. *Li^+ *initially inhibits injection, removal of* Li^+ *increases* J_{sc}	Increase	ΔG_{inj} increased by positive E_{CB} shift	Decrease	ΔG_{inj} decreased by negative E_{CB} shift. ***** Li^+ *inhibits injection.*
V_{oc}	Increase	Increased τ, no change in E_{CB}	Decrease	Positive E_{CB} shift (slightly mitigated by increased τ)	Increase	Increased τ and negative E_{CB} shift

* Hypothesis proposed here.

Mechanisms for the Changes in the Conduction Band Edge Potential, Charge Transport and Recombination Kinetics.

The major influence of the light exposure treatment across these three electrolytes appears to be a significant shift in the conduction band potential when only one cation is employed in the electrolyte. The relative conduction band positions are determined by the amount of surface charge on the TiO_2, with Li^+ having the strongest impact on this parameter since it is known to adsorb to the TiO_2 surface.[42] The negative shift in E_{CB} induced by light exposure in devices containing the Li^+ electrolyte then suggests that Li^+ is being desorbed from the surface and diffusing into the bulk of the electrolyte, since there are no negative potential determining species that could adsorb to the TiO_2. This premise is supported by the observed increase in the diffusion coefficient following light exposure. Since electron diffusion in DSSCs is typically described by an ambipolar transport mechansim, with cations from the electrolyte diffusing through the TiO_2 pores in unison with electron movement in the nanoparticles,[43]

changes in the relative concentration of ions present in the surface and bulk regions of the electrolyte will affect electron diffusion. When adsorbed to the surface, electrons may be somewhat anchored around the vicinity of the immobilized ions, which are expected to have a different diffusion coefficient to the mobile cations. Assuming the ambipolar diffusion coefficient approaches the electron diffusion coefficient at high electron densities, the electron diffusion coefficient for this electrolyte is 1.5 x 10^{-5} cm^2/s. With a lithium ion diffusion coefficient of 6 x 10^{-7} cm^2/s for the case of more mobile ions, dropping to 7 x10^{-8} cm^2/s when more of the lithium ions are immobilized on the surface, removal of 40 % of Li^+ ions from the TiO_2 surface upon light exposure would increase the ambipolar diffusion coefficient by the observed magnitude of 50% at the higher electron densities. Furthermore, the Li^+ electrolyte shows a slightly improved electron lifetime after light exposure even though the negative E_{CB} shift creates a larger free energy driving force for recombination with the redox mediator (ΔG_{recom}) and the rate of recombination is expected to show a corresponding increase.[44] This improvement in the lifetime can be explained by a movement of Li^+ ions away from the TiO_2 surface accompanied by the simultaneous movement of I_3^- ions through Coulombic attraction, thereby increasing their distance from the TiO_2 surface and decreasing the probability of reverse charge transfer.

For the case of the $DMPIm^+$ electrolyte, the positive E_{CB} shift induced in the $DMPIm^+$ electrolyte by light exposure implies that a positive potential determining species must be adsorbed to the TiO_2. The positive E_{CB} shift is attributed to a light-induced surface adsorption of $DMPIm^+$ ions. The decreased diffusion coefficient following light exposure of this electrolyte is also consistent with this cation movement since immobilization of $DMPIm^+$ ions on the TiO_2 surface would decrease the number of mobile cations participating in ambipolar diffusion. Using similar logic to that outlined for the lithium electrolyte, with an electron diffusion coefficient of 4.1 x 10^{-5} cm^2/s and ion diffusion coefficients of 1 x 10^{-6} cm^2/s for the case of more mobile ions, dropping to 1 x10^{-7} cm^2/s when more of the imidazolium ions are immobilized on the surface, removal of 35 % of $DMPIm^+$ ions from the TiO_2 surface upon light exposure would increase the ambipolar diffusion coefficient by the observed magnitude of 30% at the

higher electron densities. The increased electron lifetime is consistent with surface adsorption of $DMPIm^+$ since the positive E_{CB} shift induced by the adsorption decreases ΔG for recombination, and the bulkier $DMPIm^+$ may also have a steric blocking effect on I_3^- at the surface

The unchanged E_{CB} for the standard electrolyte can be explained by competing E_{CB} shifts as one potential determining species (Li^+) is removed from the TiO_2 surface and replaced with another ($DMPIm^+$), leading to a minimal overall change. The dipole moments of these two cations are somewhat different, and it seems unlikely that an exchange of these cations would always occur with the same ratio. Thus we note that there may be minor changes to the E_{CB} upon light exposure of different devices, but repeated measurements of ***GD2***-sensitized DSSCs within this work suggest this change is always small. The reduction in the standard electrolyte diffusion coefficient after light exposure is slightly more complex to explain, since Li^+ ions removed from the surface are replaced with adsorbed $DMPIm^+$ ions, thus the adsorbed ion concentration may be almost invariant. However, the presence of *tert*–butylpyridine (tBP) in the standard electrolyte may complex some of the mobile Li^+ ions, such that some Li^+ participate differently in ambipolar diffusion. The net effect would then be that the $DMPIm^+$ cation adsorption dominates the diffusion coefficient behaviour. The presence of tBP in the standard electrolyte could also account for the higher electron lifetime of as-prepared devices since it could act as a blocking agent on the TiO_2 surface to minimize recombination between TiO_2 electrons and the acceptor species in the electrolyte.[45] The removal of Li^+ and adsorption of $DMPIm^+$ is also consistent with the increased lifetime in the standard electrolyte following light exposure, since both effects act to increase the electron lifetime.

The increase in J_{sc} for DSSCs prepared with a standard electrolyte arises from an improved internal quantum efficiency as we have previously reported.[25] From the data in Figure 4 we have excluded an improvement in the charge collection yield since collection losses are minimal. It therefore appears that the improved photocurrent is due to either an improved injection yield, faster injection kinetics, the

prevention of a fast recombination process, or a combination of all three alternatives. Without direct kinetic measurements of the injection dynamics on fast time scales it is difficult to distinguish between these possibilities. However, for the standard electrolyte it was earlier noted that the presence of lithium ions in the electrolyte shows a lower than expected photocurrent considering the relatively high value of ΔG_{inj} for this process. In the light-induced cation exchange process we propose here, these lithium ions would be removed from the surface region, potentially removing their limitation on the injection process or promotion of a fast recombination reaction and thus increasing the J_{sc}.

III. Variation of the Electrolyte Solvent Viscosity

It was earlier noted that accumulation of electrons by application of a negative bias to the TiO_2 electrode in the dark did not reproduce the same photovoltaic improvements as the light exposure effects, and furthermore, that exposing devices to a light treatment with infrared or UV-cutoff filters produced the same results as a light treatment with the full AM 1.5 spectrum. Coupled with the strong influence of dye loading on the magnitude of light-induced performance enhancements reported in Section I, these results suggest that photo-oxidation of the dye molecules plays a crucial role in the light exposure mechanism. To investigate the effect of dye oxidation on initiation of the $DMPIm^+$ cation insertion process, the electrolyte solvent viscosity was varied to slow down the dye regeneration by I^- and alter the lifetime of oxidized dye molecules as has been previously reported.[33,46]

The photovoltaic performance parameters prior to and following light exposure of devices prepared with the 0.7 M DMPImI and 0.05 M I_2 electrolyte in various solvents (acetonitrile = ACN, methoxyacetonitrile = MeO-ACN, γ-butyrlactone = GBL and propylene carbonate = PC) are recorded in Table 3. Corresponding IPCE and *J–V* curves are displayed in Figure 7, whilst the viscosity, donor number and dielectric constants of each solvent are recorded in Table 4. The J_{sc} and V_{oc} values of as-prepared devices show a strong dependence on the electrolyte solvent. ACN-based devices show the lowest J_{sc}, whilst the higher viscosity solvents GBL and PC show a much greater photocurrent from as-

prepared devices. However, this higher current is offset by a lower V_{oc} for the GBL device, with the other three solvents showing approximately the same V_{oc}. After light exposure the ACN-based device shows the typical increase in J_{sc} and decrease in V_{oc} for the $DMPIm^+$ electrolyte. The MeO-ACN-based device shows the same trends, although the relative decrease in V_{oc} is much greater than for the ACN device. In contrast, the GBL and PC devices show large reductions in both the J_{sc} and V_{oc} following light exposure. Significant changes in the IPCE spectral shape after light exposure in these solvents, including loss of the characteristic porphyrin Q-bands and the emergence of a new absorption band around 700 nm (Figure S11) suggests this is mainly due to dye degradation under illumination.

Table 3: Photovoltaic performance parameters measured before and after light exposure for ***GD2*** DSSCs containing $DMPIm^+$ rich electrolyte II in various solvents.

Solvent	V_{oc} (mV)		J_{sc} (mA/cm^2)		Fill Factor		η (%)	
	As Prepared	Light Exposed	As Prepared	Light Exposed	As Prepared	Light Exposed	As Prepared	Light Exposed
ACN	607	580	5.24	9.11	0.597	0.646	1.90	3.41
MeO-ACN	621	382	6.51	9.31	0.675	0.570	2.73	2.03
PC	607	211	6.95	3.10	0.709	0.521	2.99	0.341
GBL	589	159	8.52	1.13	0.665	0.504	3.29	0.091

Figure 7 and Table 3 indicate that the photovoltaic performance parameters of the as-prepared GBL device are similar to those of the ACN device after light exposure. This result may imply that altering the solvent can achieve the same photovoltaic effect as light exposure for this dye. To further verify that the system properties are similar for as-prepared GBL and light exposed ACN devices, the electron lifetime and TiO_2 conduction band potentials were compared. Figures 7(b) and 7(c) indicate that the higher J_{sc} and lower V_{oc} in as-prepared devices with more viscous solvents (GBL and PC) are accompanied by longer electron lifetimes and more positive relative shifts in the TiO_2 E_{CB}. The lifetime and TiO_2 E_{CB} of the as-prepared GBL device are very similar to those of the light exposed ACN device,

confirming the photovoltaic performance data suggesting changing the solvent can produce a similar system to light exposure of ACN devices.

Table 4: Physical properties of the organic solvents employed to alter the viscosity in the $DMPIm^+$ rich electrolyte II

Solvent	Viscosity (cP)	Donor Number	Dielectric Constant
Acetonitrile (ACN)[a]	0.33	14.1	36.0
Methoxyacetonitrile (MeO-ACN)[a]	0.70	14.6	21.0
γ-butyrolactone (GBL)[b]	1.70	18.0	42.0
Propylene Carbonate (PC)[b]	2.50	15.1	65.0

[a]. Solvent properties for ACN and MeOACN taken from reference [46] and [47]
[b]. Solvent properties for GBL and PC taken from reference [48].

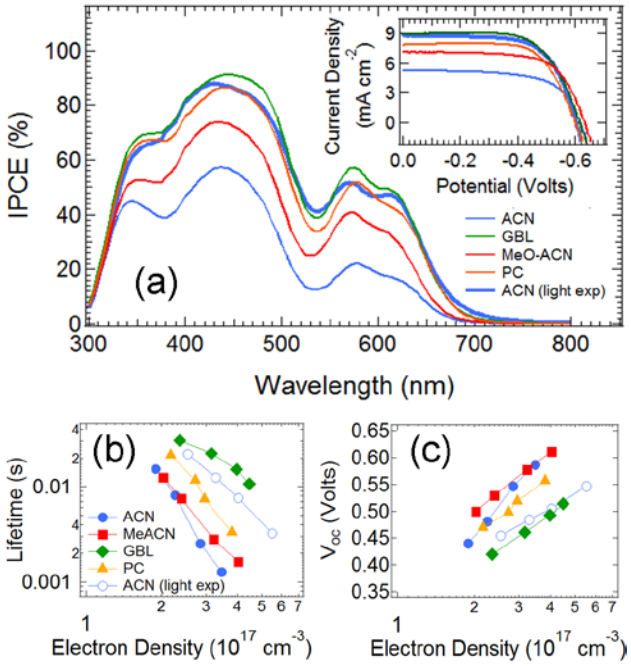

Figure 7. (a) IPCE and *J-V* curves for as-prepared devices, (b) electron lifetime versus electron density and (c) V_{oc} versus electron density for as prepared ***GD2*** DSSCs containing $DMPIm^+$ rich electrolyte II with different solvents (ACN = blue circles, MeO-ACN = red squares, GBL = green diamonds, PC = orange triangles). The respective data for a light exposed ACN device (open circles) is displayed as a reference.

It is clear that employing a solvent with higher viscosity and dielectric constant (GBL and PC) produces similar effects to those of light exposure in an ACN-based system, where the $DMPIm^+$ ions are thought

to adsorb to the TiO_2 surface. Previous reports have found that the J_{sc} and V_{oc} of devices are dependent on the donor number of the electrolyte solvent,[46,49] although in these studies, increases in V_{oc} accompanied by decreases in J_{sc} were reported when the donor number of the solvent increased, whereas the trends observed in this study are not consistent with these reports, indeed showing the opposite correlation. However, it is still possible that the donor number of the solvent affects the equilibrium constant for adsorption of electrolyte cations to the TiO_2 surface, producing different TiO_2 surface energetics as previously reported. Alternatively, given the light exposure effect is initiated by photo-oxidation of the dye molecules, it is possible that the increased solvent viscosity leads to a longer dye cation lifetime due to slower regeneration from I^-, providing an accelerated light exposure effect. To distinguish between these two effects, the lifetime and conduction band potential of devices prepared in the GBL electrolyte were measured in the dark prior to any illumination using a recently published method.[50] These values were then re-measured in the dark following acquisition of *J–V* curve, and were finally measured under illumination from a diode laser. These results are shown in Figure 8.

Figure 8(a) shows that the electron lifetime and TiO_2 E_{CB} measured in the dark prior to any illumination are different from the values re-measured in the dark following *J–V* testing and brief exposure to light. After *J–V* testing (~2 min, AM 1.5 illumination), the electron lifetime and TiO_2 E_{CB} are very similar when measured in the dark or under laser illumination. This difference in the dark lifetime measured before and after *J–V* testing suggests that the TiO_2 surface does not spontaneously form the higher performance state measured earlier in Figure 7. Instead the ~2 minutes of light exposure during *J–V* testing causes a change in the device properties, reflected by the lifetime measured in the dark and under illumination showing similar values after this *J–V* testing. Furthermore, the induced changes involve an increase in the electron lifetime and a decrease in the TiO_2 E_{CB} (Figure 8(b)), identical trends to those induced by a longer light exposure treatment for devices containing ACN solvent. These results are consistent with the same mechanism producing the high performance state in both ACN and GBL devices, with only the kinetics of the cation exchange mechanism changing for the more viscous GBL

solvent. We conclude that the solvent-dependent variation in as-prepared device performance is related to a change in the lifetime of the oxidized dye molecules in the more viscous solvent rather than different cation surface adsorption properties due to variations in the solvent donor number. This assignment is also supported by the observed dye degradation in these solvents under a prolonged light exposure treatment.

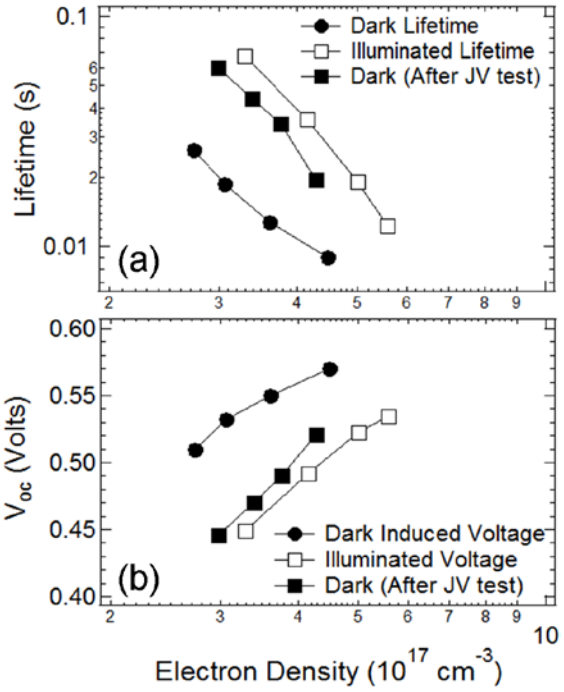

Figure 8. (a) Electron lifetime versus electron density and (b) V_{oc} versus electron density measured in the dark prior to any light exposure (solid circles), then under illumination (open squares) and in the dark (solid squares) after *J-V* measurements at AM 1.5 illumination for ***GD2*** DSSCs containing $DMPIm^+$ rich electrolyte II with GBL as a solvent

IV. Dye Structure Dependence

The cation exchange mechanism responsible for light-induced performance enhancements in ***GD2*** DSSCs is consistent with all the above measurements; however, as we have only examined this single dye it is not clear whether this cation exchange mechanism is unique to this dye or whether it can be harnessed to boost the performance of other sensitizers. To gain more insight into the Li^+ removal process and why it originally limits injection or promotes fast recombination in ***GD2*** DSSCs, a series of porphyrin dyes with different peripheral moieties and binding groups were prepared (see Figure 1) and

incorporated into DSSCs. The photovoltaic performance parameters before and after light soaking are shown in Table 5 for a porphyrin dye (***GD1***) that has a similar porphyrin core to ***GD2*** but which employs a cyanoacrylic acid binding group instead of a malonic acid group (Figure 9(a)). The electron lifetime, diffusion coefficient and TiO_2 E_{CB} values for this dye are compared to those of ***GD2***-sensitized devices prior to and following light exposure in Figure 9.

Table 5. Photovoltaic parameters measured before and after light exposure for ***GD1*** DSSCs prepared with electrolytes I, II and III

Electrolyte	V_{oc} (mV)		J_{sc} (mA/cm^2)		Fill Factor		η (%)	
	As Prepared	Light Exposed	As Prepared	Light Exposed	As Prepared	Light Exposed	As Prepared	Light Exposed
I (Standard)	567	594	4.80	4.22	0.669	0.697	1.82	1.75
II ($DMPIm^+$ rich)	503	530	2.61	6.36	0.576	0.637	0.756	2.15
III (Li^+ rich)	373	359	8.07	6.95	0.535	0.560	1.61	1.40

The trends in electron lifetime (Figure 9(c)), diffusion coefficient (Figure 9(b)) and TiO_2 E_{CB} (Figure 9(d)) are identical for ***GD1*** and ***GD2***, both in the $DMPIm^+$ electrolyte and the Li^+ electrolyte. This suggests that the cation exchange mechanism that produces these trends is common to both dyes under light exposure. In standard electrolyte, the ***GD1*** V_{oc} is enhanced by the light exposure treatment whilst the J_{sc} is decreased. The V_{oc} enhancement is consistent with the cation exchange mechanism that replaces surface Li^+ with $DMPIm^+$, a much bulkier cation which can more effectively block recombination between TiO_2 electrons and the redox mediator. In ***GD2*** devices, the light-induced photocurrent enhancement was associated with the removal of Li^+, which is suspected to inhibit the initial charge generation process. However, for ***GD1*** devices, the Li^+ electrolyte did not appear to have a negative effect on the charge generation. This can be confirmed by comparing the J_{sc} for as-prepared ***GD1*** devices with the Li^+ electrolyte (8.07 mA cm^{-2}) and light exposed devices containing the $DMPIm^+$ electrolyte (6.95 mA cm^{-2}), as was done earlier for ***GD2***-sensitized devices. For ***GD1***, the device containing the Li^+ electrolyte has a higher J_{sc}, consistent with the much more positive $E_{CB,}$ which

provides a much greater overlap between the dye LUMO and the TiO_2 acceptor orbitals, in contrast to the results observed for ***GD2***. This suggests that Li^+ ions in the surface region do not limit the injection for ***GD1*** devices, and thus the light exposure effect can be explained by the conduction band potential-dependent injection yield. In order to probe whether this was the result of the slight change in porphyrin core substitution or a result of the binder configuration, other porphyrin dyes were investigated.

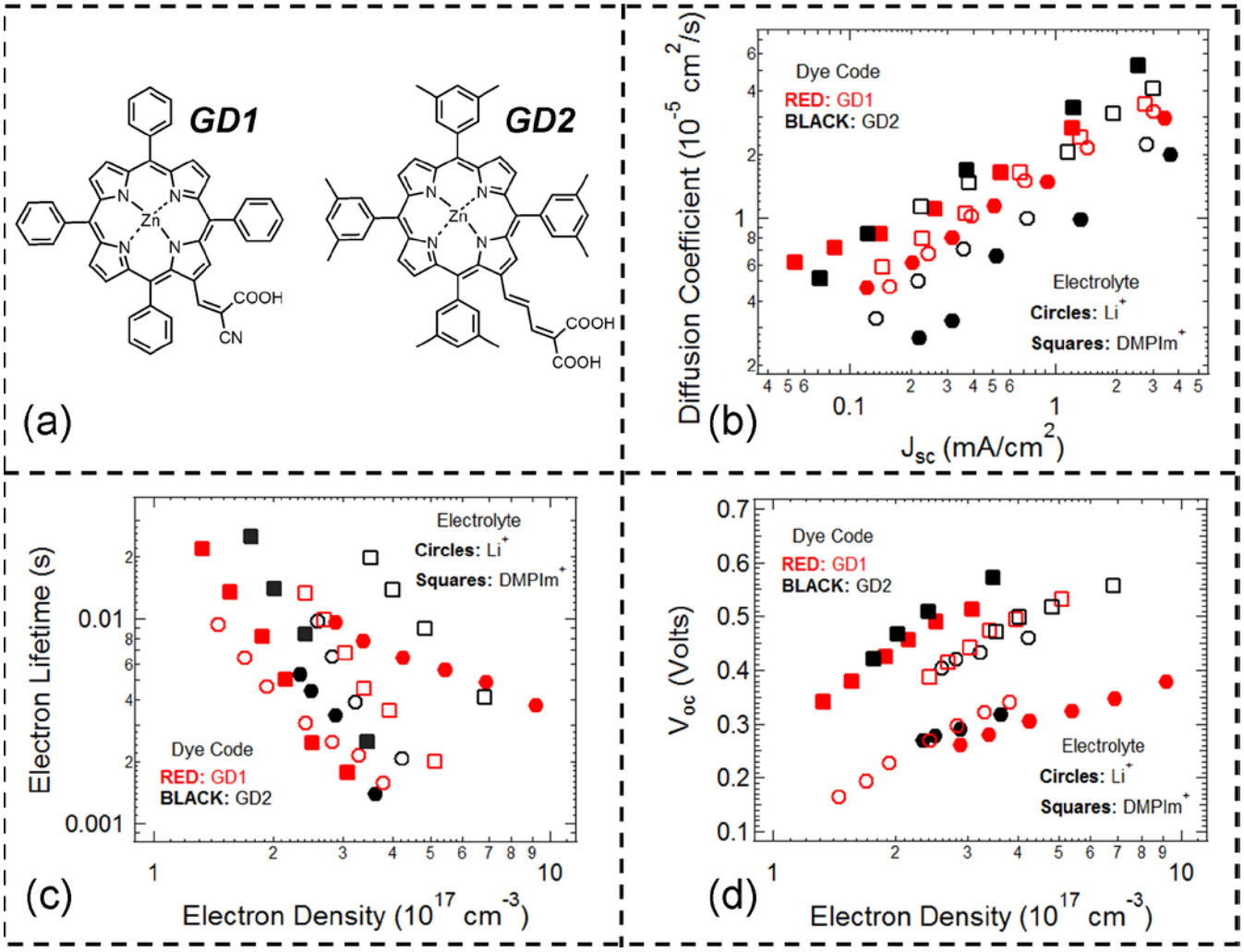

Figure 9. (a) Chemical structures, (b) diffusion coefficient vs J_{sc}, (c) electron lifetime vs electron density and (d) V_{oc} vs electron density before (solid symbols) and after (open symbols) light exposure for ***GD1*** and ***GD2*** DSSCs containing $DMPIm^+$ and Li^+ rich electrolytes.

Across several zinc porphyrin dyes tested, adding bulky tertiary-butyl (***T1***, Figure 1 and 10(a)) or even octyl substituents (***P159***, Figure 1 and 10(a)) at the *meso* position did not affect the trends in electron

lifetime (Figure 10(c)), diffusion coefficient (Figure 10(b) and TiO_2 E_{CB} (Figure 10(d)) following light exposure. These trends were always accompanied by an increased V_{oc} in standard electrolyte, consistent with the cation exchange mechanism which replaces surface Li^+ with $DMPIm^+$ (photovoltaic performance data in Tables S1-S3). However, when focusing on the binding group used to anchor the dye to the TiO_2 surface, a comparison between dyes with similar porphyrin cores but which employed either a simple carboxylic acid (***P347***, Figure 1 and 10(a)), cyanoacrylic acid (***GD1***, Figure 1 and 9(a)) or the multiple carboxylate malonic acid binding group (***GD2***, ***T1*** and ***P159***, Figure 1and 9(a)), only dyes which employed the malonic acid binder showed simultaneous J_{sc} increases after light exposure. Comparing the J_{sc} for as-prepared devices with the Li^+ electrolyte and light exposed devices containing the $DMPIm^+$ electrolyte showed that the currents scaled with changes in ΔG_{inj} for devices with a single carboxylate group only, but those with the malonic acid binding group had lower than expected J_{sc} values when the Li^+ electrolyte was employed. These results suggest that Li^+ ions either limit the injection or promote fast recombination in the dyes with a malonic acid binder, a limitation that subsequently disappears when the Li^+ is removed under light exposure.

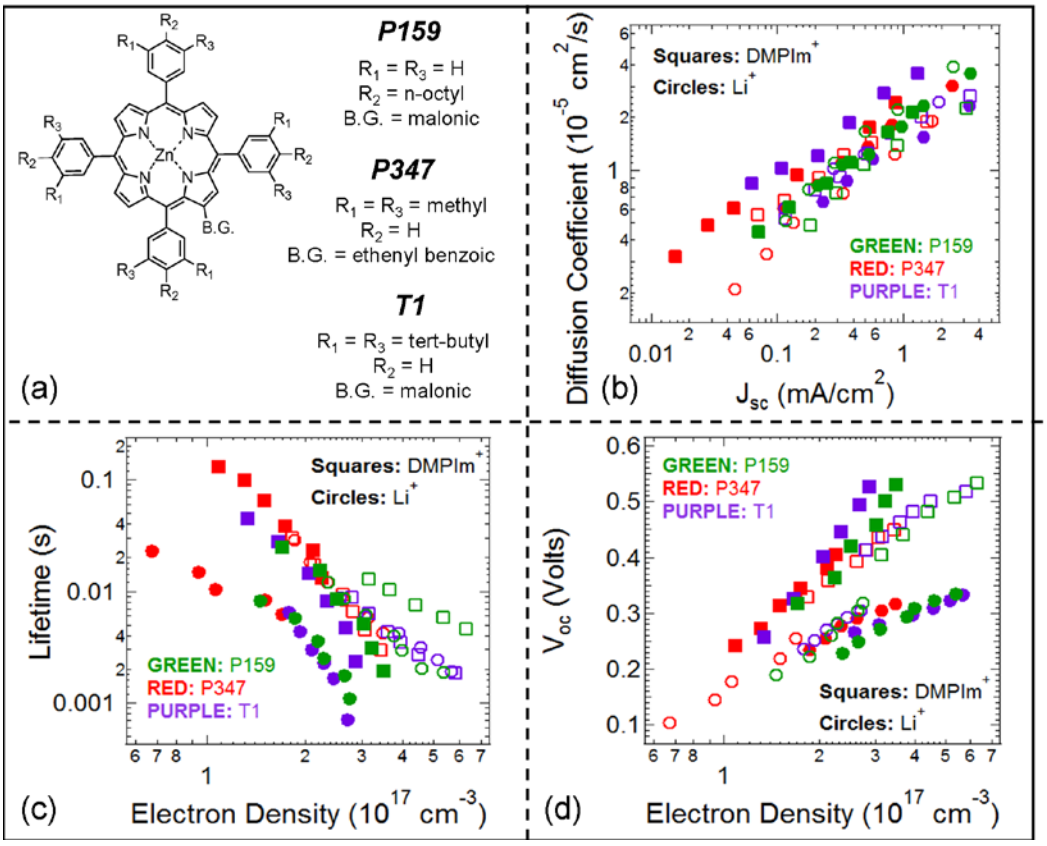

Figure 10. (a) Chemical structures, (b) diffusion coefficient vs J_{sc}, (c) electron lifetime vs electron density and (d) V_{oc} vs electron density before (solid symbols) and after (open symbols) light exposure for DSSCs prepared with various zinc porphyrin dyes and containing $DMPIm^+$ and Li^+ rich electrolytes. Note that under the light intensity giving the order of 1 ms for the lifetime, diffusion length may not be long enough and thus, the electron density obtained by charge extraction may be underestimated.

Since the charge generation limitation is only apparent for dyes that possess binding moieties with two carboxylate groups, we propose that one of these groups initially associates with Li^+ ions rather than forming a bond to the TiO_2. Upon illumination, the dye cation is created, which in turn initiates an exchange of cations at the TiO_2 surface where Li^+ ions are replaced with $DMPIm^+$ ions, as illustrated in Figure 11. Creation of the cation could repel Li^+ through either a Coulombic repulsion, or alternatively, by attracting I^- ions towards the dye with Li^+ ions then following as a counterion. Removal of the surface Li^+ species allows the second COO^- group to form a bond with the TiO_2 and either enhance injection or decrease a fast recombination process, since the $DMPIm^+$ ions are too bulky to locate themselves between the dye binding group and the TiO_2 surface and interfere with this process.

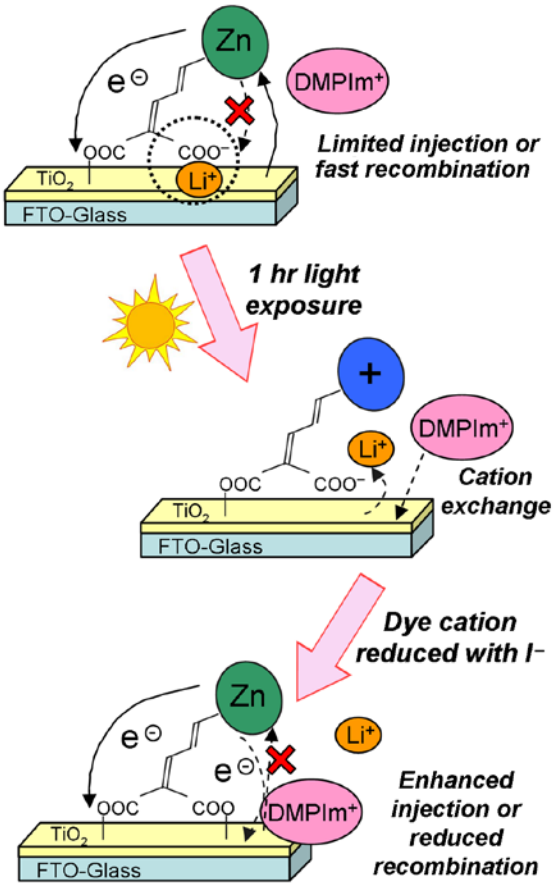

Figure 11. The proposed mechanism for simultaneous increases in the J_{sc}, V_{oc} and fill factor of ***GD2***-sensitized TiO_2 solar cells after a 1 hour light exposure treatment. Initial association of lithium with a carbonyl binding moiety limits injection or promotes fast recombination. Subsequent removal of lithium ions from the surface region under light exposure removes these limitations.

Based on these results, there appears to be general implications for other types of sensitizers exposed to light treatment. Provided there is enough open space at the surface to allow the cation exchange process observed in this study, a light treatment could be expected to lead to similar V_{oc} increases. Furthermore, for dyes which employ multiple carboxylic acid binding groups in close proximity, such as the example in this study where two carboxylic acids are connected to a to a common carbon atom on the linker frame, Li^+ ions would be expected to affect either the injection into TiO_2 or promote a fast recombination reaction. This limitation could be removed with a light exposure of these dyes, leading to improved device performance.

CONCLUSIONS

The origin of improvements in the photovoltaic performance of zinc porphyrin dye-sensitized TiO_2 solar cells under white light illumination has been elucidated. Detailed examinations of photovoltage and photocurrent transients for devices prepared using various electrolyte compositions have indicated that enhancements in the J_{sc} and V_{oc} are consistent with a light-induced exchange of cations in the electrolyte. Under illumination, Li^+ ions are removed from the TiO_2 surface and replaced with $DMPIm^+$ ions, a process which enhances the electron lifetime by decreasing recombination with the redox mediator. Similar effects were not replicated by application of negative bias under dark conditions. Variation of the electrolyte solvent viscosity indicated that the performance of devices could be increased to levels close to those achieved after light exposure in acetonitrile, with subsequent comparisons of the electron lifetime in the dark and under illumination revealing that these changes reflected an accelerated rate of light-induced performance enhancements in more viscous solvents. These results were consistent with a light exposure effect initiated by formation of dye cation molecules following photo-excitation rather than photoinduced changes in the semiconductor surface states. The peripheral moiety and type of linker group on the porphyrin chromophore were both varied in order to investigate the structural features of the dyes which make them susceptible to light-induced improvements in the J_{sc}. Enhanced J_{sc} as a result of light exposure was only measured for dyes possessing two carboxylic acid binding groups, a feature arising from the light-induced removal of the Li^+ that initially either limits injection or promotes fast recombination at the dye/TiO_2 interface. We conclude that light exposure may produce increases in the V_{oc} of dyes with open space at the TiO_2 surface, such as planar or poorly stacked molecules, due to the electrolyte cation exchange. For dyes that employ multiple carboxylate binding groups and show charge generation limitations such as the porphyrins studied here, simultaneous improvements in J_{sc} may also be possible.

ACKNOWLEDGEMENT

The support of the Australian Research Council through the ARC Center of Excellence, Federation Fellowship, Discovery, and LIEF schemes is gratefully acknowledged. *MJG* acknowledges the support of a Prime Minister's Australia Asia Endeavour Award from the Australian Department of Education, Employment and Workplace Relations.

SUPPORTING INFORMATION AVAILABLE

The change in V_{oc}, J_{sc} and fill factor observed for ***GD2***-sensitzed solar cells containing $DMPIm^+$ rich electrolyte II after application of an external bias in the dark for 1 hour (Figure S1). The dependence of V_{oc} on the light intensity, and the electron lifetime on device V_{oc} for selected ***GD2*** devices prior to and following light exposure (Figure S6). Photocurrent, photovoltage and extracted charge transients prior to and following light exposure for devices prepared with electrolytes I (Figures S2-S5), II (Figure S7-S8) and III (Figure S9-S10). IPCE curves following light exposure of devices prepared using electrolyte II in various solvents (Figure S11). This information is available free of charge via the Internet at http://pubs.acs.org

REFERENCES

(1) O'Regan, B.; Grätzel, M., A Low-Cost, High-Efficiency Solar Cell Based on Dye-Sensitized Colloidal TiO_2 Films, *Nature*, **1991**, *353*, 737-740.

(2) Hagfeldt, A.; Gratzel, M., Light-Induced Redox Reactions in Nanocrystalline Systems, *Chem. Rev.*, **1995**, *95*, 49-68.

(3) Grätzel, M., Dye Sensitized Solar Cells, *J. Photochem. Photobiol. C*, **2003**, *4*, 145-153.

(4) Haque, S. A.; Palomares, E.; Cho, B. M.; Green, A. N. M.; Hirata, N.; Klug, D. R.; Durrant, J. R., Charge Separation Versus Recombination in Dye Sensitized Solar Cells: The Minimization of Kinetic Redundancy, *J. Am. Chem. Soc.*, **2005**, *127*, 3456-3462.

(5) Chiba, Y.; Islam, A.; Watanabe, Y.; Komiya, R.; Koide, N.; Han, L., Dye Sensitized Solar Cells With Conversion Efficiency of 11.1%, *Jap. J. App. Phys.*, **2006**, *45*, L638-L640.

(6) Yu, Q.; Wang, Y.; Yi, Z.; Zu, N.; Zhang, J.; Zhang, M.; Wang, P., High-Efficiency Dye-Sensitized Solar Cells: The Influence of Lithium Ions on Exciton Dissociation, Charge Recombination and Surface States, *ACS Nano*, **2010**, *4*, 6032-6038.

(7) Yella, A.; Lee, H.-W.; Tsao, H. N.; Yi, C.; Chandiran, A. K.; Nazeeruddin, M. K.; Diau, E. W.-G.; Yeh, C.-Y.; Zakeeruddin, S. M.; Grätzel, M., Porphyrin-Sensitized Solar Cells with Cobalt (II/III)–Based Redox Electrolyte Exceed 12 Percent Efficiency, *Science*, **2011**, *334*, 629-634.

(8) Bessho, T.; Zakeeruddin, S. M.; Yeh, C.-Y.; Diau, E. W.-G.; Grätzel, M., Highly Efficient Mesoscopic Dye-Sensitized Solar Cells Based on Donor–Acceptor-Substituted Porphyrins, *Angew. Chem. Int. Ed.*, **2010**, *49*, 6646-6649.

(9) Campbell, W. M.; Burrell, A. K.; Officer, D. L.; Jolley, K. W., Porphyrins as Light Harvesters in the Dye Sensitized Solar Cell, *Coord. Chem. Rev.*, **2004**, *248*, 1363-1379.

(10) Dos Santos, T.; Morandeira, A.; Koops, S.; Mozer, A. J.; Tsekouras, G.; Dong, Y.; Wagner, P.; Wallace, G.; Earles, J. C.; Gordon, K. C.; Officer, D. L.; Durrant, J. R., Injection Limitations in a Series of Porphyrin Dye Sensitized Solar Cells, *J. Phys. Chem. C*, **2010**, *114*, 3276-3279.

(11) Koehorst, R. B. M.; Boschloo, G. K.; Savenije, T. J.; Goossens, A.; Schaafsma, T. J., Spectral Sensitization of TiO_2 Substrates by Monolayers of Porphyrin Heterodimers, *J. Phys. Chem. B*, **2000**, *104*, 2371-2377.

(12) Mozer, A. J.; Griffith, M. J.; Tsekouras, G.; Wagner, P.; Wallace, G. G.; Mori, S.; Sunahara, K.; Miyashita, M.; Earles, J. C.; Gordon, K. C.; Du, L.; Katoh, R.; Furube, A.; Officer, D. L., Zn-Zn Porphyrin Dimer-Sensitised Solar Cells: Towards 3-D Light Harvesting, *J. Am. Chem. Soc.*, **2009**, *131*, 15621-15623.

(13) Lin, C.-Y.; Lo, C.-F.; Luo, L.; Lu, H.-P.; Hung, C.-S.; Diau, E. W.-G., Design and Characterization of Novel Porphyrins with Oligo(phenylethylnyl) Links of Varied Length for Dye-Sensitized Solar Cells: Synthesis and Optical, Electrochemical, and Photovoltaic Investigation, *J. Phys. Chem. C*, **2009**, *113*, 755-764.

(14) Imahori, H., Porphyrins as Potential Sensitizers for Dye Sensitized Solar Cells, *Key Eng. Mater.*, **2010**, *451*, 29-40.

(15) Clifford, J. N.; Forneli, A.; Chen, H.; Torres, T.; Tan, S.; Palomares, E., Co-Sensitized DSCs: Dye Selection Criteria for Optimized Device V_{oc} and Efficiency, *J. Mater. Chem.*, **2011**, *21*, 1693-1696.

(16) Imahori, H.; Umeyama, T.; Ito, S., Large π-aromatic Molecules as Potential Sensitizers for Highly Efficient Dye Sensitized Solar Cells, *Acc. Chem. Res.*, **2009**, *42*, 1809-1818.

(17) Liu, Y.; Lin, H.; Dy, J. T.; Tamaki, K.; Nakazaki, J.; Nakayama, D.; Uchida, S.; Kubo, T.; Segawa, H., N-fused Carbazole–Zinc Porphyrin–Free-Base Porphyrin Triad for Efficient Near-IR Dye-Sensitized Solar Cells, *Chem. Comm.*, **2011**, *47*, 4010-4012.

(18) Mozer, A. J.; Wagner, P.; Officer, D. L.; Wallace, G. G.; Campbell, W. M.; Miyashita, M.; Sunaharac, K.; Mori, S., The Origin of Open Circuit Voltage of Porphyrin-Sensitised TiO_2 Solar Cells, *Chem. Comm.*, **2008**, 4741-4743.

(19) Imahori, H.; Kang, S.; Hayashi, H.; Haruta, M.; Kurata, H.; Isoda, S.; Canton, S. E.; Infahsaeng, Y.; Kathiravan, A.; Pascher, T.; Chabera, P.; Yartsev, A. P.; Sundstrom, V., Photoinduced Charge Carrier Dynamics of Zn-Porphyrin-TiO_2 Electrodes: The Key Role of Charge Recombination for Solar Cell Performance, *J. Phys. Chem. A*, **2011**, *115*, 3679-3690.

(20) Griffith, M. J.; Sunahara, K.; Wagner, P.; Wagner, K.; Wallace, G. G.; Officer, D. L.; Furube, A.; Katoh, R.; Mori, S.; Mozer, A. J., Porphyrins for Dye-Sensitised Solar Cells: New Insights into Efficiency-Determining Electron Transfer Steps, *Chem. Comm.*, **2012**, *48*, 4145-4162.

(21) Forneli, A.; Planells, M.; Angele, M.; Sarmentero; Martinez-Ferrero, E.; O'Regan, B. C.; Ballester, P.; Palomares, E., The Role of Para-Alkyl Substituents on Meso-Phenyl Porphyrin Sensitised

TiO_2 Solar Cells: Control of the e_{TiO2}/Electrolyte$^+$ Recombination Reaction, *J. Mater. Chem.*, **2008**, *18*, 1652-1658.

(22) Imahori, H.; Matsubara, Y.; Iijima, H.; Umeyama, T.; Matano, Y.; Ito, S.; Niemi, M.; Tkachenko, N. V.; Lemmetyinen, H., Effects of Meso-Diarylamino Group of Porphyrins as Sensitizers in Dye Sensitized Solar Cells on Optical, Electrochemical, and Photovoltaic Properties, *J. Phys. Chem. C*, **2010**, *114*, 10656-10665.

(23) Hsieh, C.-P.; Lu, H.-P.; Chiu, C.-L.; Lee, C.-W.; Chuang, S.-H.; Mai, C.-L.; Yen, W.-N.; Hsu, S.-J.; Diau, E. W.-G.; Yeh, C.-Y., Synthesis and Characterization of Porphyrin Sensitizers With Various Electron-Donating Substituents for Highly Efficient Dye-Sensitized Solar Cells, *J. Mater. Chem.*, **2010**, *20*, 1127-1134.

(24) Stromberg, J. R.; Marton, A.; Kee, H. L.; Kirmaier, C.; Diers, J. R.; Muthiah, C.; Taniguchi, M.; Lindsey, J. S.; Bocian, D. F.; Meyer, G. J.; Holten, D., Examination of Tethered Porphyrin, Chlorin, and Bacteriochlorin Molecules in Mesoporous Metal-Oxide Solar Cells, *J. Phys. Chem. C*, **2007**, *111*, 15464-15478.

(25) Wagner, K.; Griffith, M. J.; James, M.; Mozer, A. J.; Wagner, P.; Triani, G.; Officer, D. L.; Wallace, G. G., Significant Performance Improvement of Porphyrin-Sensitised TiO_2 Solar Cells Under White Light Illumination, *J. Phys. Chem. C*, **2011**, *115*, 317-326.

(26) Wang, Q.; Zhang, Z.; Zakeeruddin, S. M.; Grätzel, M., Enhancement of the Performance of Dye Sensitized Solar Cells by Formation of Shallow Transport Levels Under Visible Light Illumination, *J. Phys. Chem. C*, **2008**, *112*, 7084-7092.

(27) Gregg, B. A.; Chen, S.-G.; Ferrere, S., Enhanced Dye-Sensitized Photoconversion Efficiency via Reversible Production of UV-Induced Surface States in Nanoporous TiO_2, *J. Phys. Chem. C*, **2003**, *107*, 3019-3029.

(28) Sauvage, F.; Fischer, M. K. R.; Mishra, A.; Zakeeruddin, S. M.; Nazeeruddin, M. K.; Bäuerle, P.; Grätzel, M., A Dendritic Oligothiophene Ruthenium Sensitizer for Stable Dye Sensitized Solar Cells, *Chem. Sus. En. Mater.*, **2009**, *2*, 761-768.

(29) Listorti, A; Creager, C; Sommeling, P; Kroon, J; Palomares, E; Fornelli, A; Breen, B; Barnes, P. R. F; Durrant, J. R; Law, C; O'Regan, B., The Mechanism Behind the Beneficial Effect of Light Soaking on Injection Efficiency and Photocurrent in Dye Sensitized Solar Cells, *Ener. Environ. Sci.*, **2011**, *4*, 3494-3501.

(30) Campbell, W. M.; Jolley, K. W.; Wagner, P.; Wagner, K.; Walsh, P. J.; Gordon, K. C.; Schmidt-Mende, L.; Nazeeruddin, M. K.; Wang, Q.; Grätzel, M.; Officer, D. L., Zn Porphyrins as Highly Efficient Sensitizers in Dye Sensitized Solar Cells, *J. Phys. Chem. C*, **2007**, *111*, 11760-11762.

(31) Wang, Q.; Campbell, W. M.; Bonfantani, E. E.; Jolley, K. W.; Officer, D. L.; Walsh, P. J.; Gordon, K.; Humphry-Baker, R.; Nazeeruddin, M. K.; Grätzel, M., Efficient Light Harvesting by Using Green Zn-Porphyrin-Sensitized Nanocrystalline TiO_2 Films, *J. Phys. Chem. B*, **2005**, *109*, 15397-15409.

(32) Ito, S.; Nazeeruddin, M. K.; Liska, P.; Comte, P.; Charvet, R.; Pechy, P.; Jirousek, M.; Kay, A.; Zakeeruddin, S. M.; Grätzel, M., Photovoltaic Characterization of Dye Sensitized Solar Cells: Effect of Device Masking on Conversion Efficiency, *Prog. Photovol. Res. App.*, **2006**, *14*, 589-601.

(33) Nakade, S.; Kanzaki, T.; Wada, Y.; Yanagida, S., Stepped Light-Induced Transient Measurements of Photocurrent and Voltage in Dye Sensitized Solar Cells: Application for Highly Viscous Electrolyte Systems, *Langmuir*, **2005**, *21*, 10803-10807.

(34) Duffy, N. W.; Peter, L. M.; Rajapakse, R. M. G.; Wijayantha, K. G. U., A Novel Charge Extraction Method for the Study of Electron Transport and Interfacial Transfer in Dye Sensitised Nanocrystalline solar Cells, *Electrochem. Comm.*, **2000**, *2*, 658-662.

(35) Wang, H.; Peter, L. M., A Comparison of Different Methods To Determine the Electron Diffusion Length in Dye-Sensitized Solar Cells, *J. Phys. Chem. C*, **2009,** *113*, 18125-18133.

(36) Furube, A.; Katoh, R.; Hara, K.; Sato, T.; Murata, S.; Arakawa, H.; Tachiya, M., Lithium Ion Effect on Electron Injection from a Photoexcited Coumarin Derivative into a TiO_2 Nanocrystalline Film Investigated by Visible-to-IR Ultrafast Spectroscopy, *J. Phys. Chem. B*, **2005**, *109*, 16406-16414.

(37) Bisquert, J; Mora-Seró, I., Simulation of Steady-State Characteristics of Dye-Sensitized Solar Cells and the Interpretation of the Diffusion Length, *J. Phys. Chem. Lett.*, **2010**, *1*, 450-456.

(38) Jennings, J.R.; Li F.; Wang, Q., Reliable Determination of Electron Diffusion Length and Charge Separation Efficiency in Dye-Sensitized Solar Cells, *J. Phys. Chem. C*, **2010**, *114*, 14665-14674.

(39) Kambe, S.; Nakade, S.; Kitamura, T.; Wada, Y.; Yanagida, S., Influence of the Electrolytes on Electron Transport in Mesoporous TiO_2−Electrolyte Systems, *J. Phys. Chem. B*, **2002**, *106*, 2967-2972.

(40) Kopidakis, N.; Neale, N. R.; Frank, A. J., Effect of an Adsorbent on Recombination and Band-Edge Movement in Dye-Sensitized TiO_2 Solar Cells: Evidence for Surface Passivation, *J. Phys. Chem. B*, **2006**, *110*, 12485-12489.

(41) Liu, Y.; Hagfeldt, A.; Xiao, X.-R.; Lindquist, S.-E., Investigation of Influence of Redox Species on the Interfacial Energetics of a Dye-Sensitized Nanoporous TiO_2 Solar Cell, *Sol. En. Mater. Sol. Cells*, **1998**, *55*, 267-281.

(42) Kopidakis, N.; Benkstein, K.D.; van de Lagemaat, J.; Frank, A. J., Transport-Limited Recombination of Photocarriers in Dye-Sensitized Nanocrystalline TiO_2 Solar Cells, *J. Phys. Chem. B*, **2003**, *107*, 11307-11315.

(43) Kopidakis, N.; Schiff, E. A.; Park, N.-G.; J. van de Lagemaat; Frank, A. J., Ambipolar Diffusion of Photocarriers in Electrolyte-Filled, Nanoporous TiO2, *J. Phys. Chem. B*, **2000**, *104*, 3930-3936.

(44) Miyashita, M.; Sunahara, K.; Nishikawa, T.; Uemura, Y.; Koumura, N.; Hara, K.; Mori, A.; Abe, T.; Suzuki, E.; Mori, S., Interfacial Electron-Transfer Kinetics in Metal-Free Organic Dye-Sensitized Solar Cells: Combined Effects of Molecular Structure of Dyes and Electrolytes, *J. Am. Chem. Soc.*, **2008**, *130*, 17874-17881.

(45) Boschloo, G.; Häggman, L.; Hagfeldt, A., Quantification of the Effect of 4-tert-Butylpyridine Addition to I^-/I_3^- Redox Electrolytes in Dye-Sensitized Nanostructured TiO_2 Solar Cells, *J. Phys. Chem. B*, **2006**, *110*, 13144-13150.

(46) Montanari, I.; Nelson, J.; Durrant, J. R., Iodide Electron Transfer Kinetics in Dye-Sensitized Nanocrystalline TiO_2 Films, *J. Phys. Chem. B*, **2002**, *106*, 12203-12210.

(47) Fukui, A.; Komiya, R.; Yamanaka, R.; Islam, A.; Han, L., Effect of a Redox Electrolyte in Mixed Solvents on the Photovoltaic Performance of a Dye-Sensitized Solar Cell, *Sol. En. Mater. Sol. Cells*, **2006**, *90*, 649-658.

(48) Nazeeruddin, M. K.; Péchy, P.; Renouard, T.; Zakeeruddin, S. M.; Humphry-Baker, R.; Comte, P.; Liska, P.; Cevey, L.; Costa, E.; Shklover, V.; Spiccia, L.; Deacon, G. B.; Bignozzi, C. A.; Grätzel, M., Engineering of Efficient Panchromatic Sensitizers for Nanocrystalline TiO_2-Based Solar Cells, *J. Am. Chem. Soc.*, **2001**, *123*, 1613-1624.

(49) Wu, J.; Lan, Z.; Lin, J.; Huang, M.; Li, P., Effect of Solvents in Liquid Electrolyte on the Photovoltaic Performance of Dye-Sensitized Solar Cells, *J. Power Source*, **2007**, *173*, 585-591.

(50) Sunahara, K.; Ogawa, J.; Mori, S., A Method to Measure Electron Lifetime in Dye-Sensitized Solar Cells: Stepped Current Induced Measurement of Cell Voltage in the Dark, *Electrochem. Comm.*, **2011**, *13*, 1420-1422.

TABLE OF CONTENTS GRAPHIC: